Theoretical model for VITA-educed coherent structures in the wall region of a turbulent boundary layer

By Marten T. Landahl[1]

1 Introduction

Experiments on wall-bounded shear flows (channel flows and boundary layers) have indicated that the turbulence in the region close to the wall exhibits a characteristic pattern of intermittently formed coherent structures. This was first clearly demonstrated in the visualization experiments of Kline et al.(1967), in which it was seen that most of the turbulence generation takes place during randomly recurring, comparatively short-time, bursting events in the near-wall region (in the viscous and buffer layers) separated by periods of unsteady, but basically inactive, quasi-laminar motion. The coherent structures have been found to carry a major portion of the turbulent stress.

For a quantitative study of coherent structures it is necessary to make use of conditional sampling. One particularly successful sampling technique is the Variable Integration Time Averaging technique (VITA) first explored by Blackwelder and Kaplan (1976). In this, an event is assumed to occur when the short-time variance exceeds a certain threshold multiple of the mean square signal. This sampling technique has been found to bring out structures characterized by a low-speed (downstream) region and a high-speed (upstream) one separated by a thin, inclined shear layer. The measurements by Johansson and Alfredsson (1982) showed that the rate of occurrence of such structures ("bursting rate") varies with the integration time and threshold parameter selected. The most frequently found structures have streamwise lengths of the order of a few hundred viscous wall units. In the original work on the modelling of the VITA structures (Landahl, 1984a; 1984b) the structure was assumed to be initiated by a local inflectional type instability producing a transient disturbance, localized in space and time, the evolution of which was then followed by application of an approximate linear theory in which the effects due to viscosity and streamwise pressure gradient were neglected. This theory was found to give results for the sampled velocity signatures in good qualitative agreement with the experiments.

The analysis presented here removes some of the assumptions in the earlier models in that the effects of pressure and viscosity are taken into account in an approximation based on the assumption that the near- wall structures are highly elongated in the streamwise direction. The appropriateness of this is suggested by the observations but is also self consistent with the results of the model which show that the

1 Massachusetts Institute of Technology

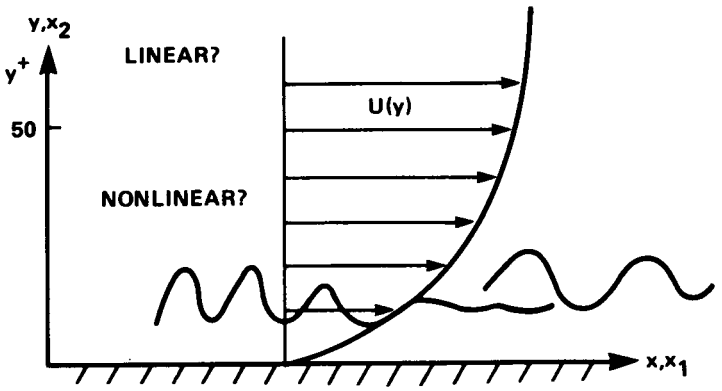

FIGURE 1. Coordinate system and definitions.

streamwise dimension of the structure grows with time, so that the approximation should improve with the age of the structure.

2. Analysis

Basic assumptions in the analysis are that the mean flow is parallel and that the nonlinearity is intermittent. Denoting by $U(x_2)(x_2 = y)$ the mean velocity, by $u_i(x_j, t)$ the fluctuating velocity, and by p the fluctuating part of the pressure (see Figure 1). Navier-Stokes equations give the following set of equations for the fluctuating velocity field

$$\frac{Du_j}{Dt} - vU'\delta_{i1} = -\frac{\partial p}{\partial x_i} + \nu\nabla^2 v + T_i \tag{1}$$

where

$$Ti = \frac{\partial \tau_{ij}}{\partial x_j} \tag{2}$$

and where

$$\tau_{ij} = -\rho(u_i u_j - \overline{u_i u_j}) \tag{3}$$

are the "fluctuating Reynolds stresses", overbar denoting average.

Elimination of the pressure with the aid of the continuity equation,

$$\frac{\partial u_i}{\partial x_i} = 0 \tag{4}$$

gives the following equation for the vertical velocity component:

$$D(\nabla^2 v)/Dt - \frac{\partial v}{\partial x}U'' - \nu\nabla^4 v = q \tag{5}$$

where

$$q = \nabla^2 T_2 - \frac{\partial^2 T_i}{\partial x_i \partial x_2} \tag{6}$$

and where

$$T_i = \frac{\partial \tau_{ij}}{\partial x_j} \tag{7}$$

For infinitesimal fluctuating velocity amplitudes the right-hand side of (7) may be neglected, and one recovers the Orr-Sommerfeld equation (in physical space) for the v-component.

On the anticipation that the structures to be analyzed have a boundary layer character in the sense that their vertical dimensions are much smaller than their horizontal ones, the dominating terms in the expression for q would be those having the highest-order y- derivatives, namely

$$< q > \cong -(\frac{\partial^2}{\partial y^2})[\frac{\partial(uv)}{\partial x} - \frac{\partial(vw)}{\partial z}] \quad + \quad \text{higher order horiz. derivatives} \tag{8}$$

For such eddies, we will determine an approximate inviscid solution valid for small y (i.e., small compared to the largest horizontal dimensions of the eddy). We write the equation as follows:

$$\frac{D\phi}{Dt} - \nu\nabla^2\phi = q_1 \tag{9}$$

where

$$\phi = \nabla^2 v \tag{10}$$

$$q_1 = q + U''\frac{\partial v}{\partial x} \tag{11}$$

In the inviscid limit ($\nu = 0$) the formal solution of (9) is given by

$$\phi = \int_{-\infty}^{t} q_1(\xi_1; y; z, t_1)dt_1 \tag{12}$$

where

$$\xi_1 = x - U(y)(t - t_1) \tag{13}$$

On the anticipation that most of the structures of special interest are highly elongated in the streamwise direction and thus vary slowly in the x-direction, we will, for simplicity in the analysis, include only the terms originating from the lowest-order x-derivatives. Hence, the term on the right-hand side of (11) proportional to U'' will be neglected in the following. Of course, this is only allowed if U'' does not change sign anywhere, because then an inflectional-type instability may produce an exponentially growing wave for which the term is essential. The inviscid solution (12) then simplifies to

$$\phi = \int_{-\infty}^{t} q(\xi_1; y; z, t_1)dt_1 \tag{14}$$

The solution for v is obtained by solving the Poisson equation (10). Application of Fourier transform in the x, z-plane gives, with 'tilde' denoting transformed quantities, $k = \alpha^2 + \beta^2$, α and β being the transform variables in x and z, respectively,

$$\tilde{v} = -\frac{1}{2k}\int_0^\infty [e^{-k|y-y_1|} - e^{-k(y+y_1)}]\tilde{\phi}(y_1)dy_1 \tag{15}$$

where the second term under the integral sign is selected so as to give $\tilde{v} = 0$ on the wing. For values of y that are small compared to the horizontal dimensions of the structure, and for a structure with a small vertical extent compared to its horizontal dimensions ("flat eddy"), (14) may be expanded to yield, to lowest order in y,

$$\tilde{v} \cong \frac{1}{2}\int_0^\infty (|y - y_1| - y - y_1)\tilde{\phi}(\xi, y_1; z, t_1)dy_1 \equiv \tilde{v}_f \tag{16}$$

or, in the physical plane,

$$v_f = \frac{1}{2}\int_0^\infty (|y - y_1| - y - y_1)\phi(\xi_1, y_1; z, t_1)dy_1 \tag{17}$$

It follows from (17) that the streamwise size of the disturbed region from an initial disturbance grows linearly in time at a rate $U_{\max} - U_{\min}$, where $U_{\max}$ and $U_{\min}$ are, respectively, the maximum and the minimum velocities of the mean flow.

For a structure with vertical and spanwise dimensions both small compared to the streamwise dimension ("sausage eddy") the appropriate approximation is found by replacing k by $|\beta|$ in (15). Upon inversion this yields

$$v = \frac{1}{2\pi}\int_0^\infty dy_1 \int_{-\infty}^\infty \phi(\xi_1, y_1, z_1, t_1)\log(\frac{r_1}{r_2})dz_1 \equiv v_s \tag{18}$$

If q is intermittent so that it is zero for $t > t_o$, say, then for the flat-eddy approximation (17) for $t > t_o$,

$$v_f = \frac{1}{2}\int_0^\infty (|y - y_1| - y - y_1)\phi_o(\xi, y_1; z)dy_1 \tag{19}$$

where $\xi = x - (t - t_o)U(y_1)$ and where

$$\phi_o(\xi, y; z) = \nabla^2 v_o = \int_{-\infty}^{t_o} q(\xi'; y; z, t_1)dt_1 \tag{20}$$

where $\xi' = \xi + U(y)(t_1 - t_o)$. Similarly, for the "sausage" approximation (18)

$$v_s = \frac{1}{2\pi}\int_0^\infty dy_1 \int_{-\infty}^\infty \phi_o(\xi, y_1, z_1, t_1)\log(\frac{r_1}{r_2})dz_1 \tag{21}$$

It follows from (19)-(21) that, for any smooth function ϕ_o, the vertical velocity will decay like t^{-1} as $t \to \infty$ when q is intermittent.

The streamwise component u satisfies

$$\frac{Du}{Dt} = -\frac{\partial p}{\partial x} - vU' - \nu\nabla^2 u + q_u \tag{22}$$

where q_u stands for the nonlinear terms. In accordance with the intermittency assumption of the nonlinear terms, we assume that q_u is negligible for $t > t_o$. At large times the coherent structure becomes highly elongated so that $\partial p/\partial x$, as well, becomes negligible. With the additional assumptions that $u = 0$ for $t = t_o$, the inviscid solution for u then becomes

$$u = -U'(y)lm \tag{23}$$

where

$$l_m = \int_{-\infty}^{t} v(\xi_1; y; z, t_1)dt_1 \tag{24}$$

is the vertical displacement (in linearized approximation) of the fluid element from its initial undisturbed position at $t = -\infty$. This result is equivalent to that proposed Prandtl (1925) in his mixing- length theory, see Landahl (1984b).

After application of conditional sampling to the above equations they may then be used for the study of coherent structures. For this purpose it is necessary to select a suitable model for the the nonlinear driving terms represented by q.

3. Statistical model for the nonlinear driving term

Since the coherent structures are intermittent, and hence well separated in time and space, they may be regarded as statistically independent. Upon application of conditional sampling to the nonlinear terms one could therefore expect the sampled stress term $< q >$ (angular brackets denoting conditionally sampled quantities) to give results varying with time and horizontal distances like a Gaussian "hat". For a coherent structure which is symmetrical in the z-direction, one would expect $< vw >$ to be zero. Thus, the term involving $< vw >$ may be neglected and from (7) it follows that an expression of the form

$$< \tau_{11} >= f(y)[1 - 2(\frac{z}{l_3})^2]\exp[-(\frac{x}{l_1})^2 - (\frac{z}{l_3})^2 - (\frac{\tau}{t_b})^2] \tag{25}$$

where l_1 ,l_3, and t_b are, respectively, the streamwise, spanwise, and time scales of the burst, and where $\tau = t - t_o$, would give an appropriate representation of the nonlinear driving term. The function of z multiplying the exponential is selected so as to make

$$\int_{-\infty}^{\infty} < \tau_{11} > dz_1 = 0 \tag{26}$$

since otherwise the resulting disturbance will not vanish for large $|z|$, i.e., will not be a localized one.

The dependence on y cannot be found by such simple reasoning; therefore, we make use here of the model proposed by Bark (1975),

$$f(y) = C(\frac{y}{l_2})^3\exp[-(\frac{y}{l_2})^2] \tag{27}$$

C being a constant (not needed, see below), which, with the vertical scale l_2 chosen to be 15 in viscous wall units, gives a good fit to the Reynolds stress distribution during bursting found in the measurements by Kim et al. (1972). In the following treatment we shall adopt the simple model that the nonlinear terms are highly intermittent so that we set $t_b \approx 0$. Thus, upon insertion in (20) we find

$$\phi_o = K[1 - 2(\frac{z}{l_3})^2](\frac{\partial}{\partial \xi})\exp[-(\frac{\xi}{l_1})^2 - (\frac{y}{l_2})^2 - (\frac{z}{l_3})^2] \tag{28}$$

where K is a numerical constant measuring the integrated strength of the nonlinear driving term.

4. Correction for long-time viscous effects

From (22) we have for long times when $v \to 0$ and the nonlinear and viscous effects are negligible

$$\frac{Du}{Dt} \approx 0 \tag{29}$$

Thus, as $t \to \infty$

$$u(x, y, z, t) \to u_\infty(\xi; y; z) \tag{30}$$

where $\xi = x - (t - t_o)U(y)$. However, viscous diffusion will become important for large times when u must satisfy

$$\frac{Du}{Dt} - \nu \nabla^2 u = 0 \tag{31}$$

By introducing the convected coordinate ξ by setting

$$u = u(\xi, y, z, t) \tag{32}$$

one finds that

$$\nabla^2 u = t^2[U'(y)]^2 \frac{\partial^2 u}{\partial \xi^2} - 2tU'(y)\frac{\partial^2 u}{\partial \xi \partial y} - tU''(y)\frac{\partial u}{\partial \xi} \tag{33}$$

Hence, as t becomes large,

$$\frac{\partial u}{\partial t} - vt^2[U'(y)]^2 \frac{\partial^2 u}{\partial \xi^2} + (\text{higher order terms in } t^{-1}) = 0 \tag{34}$$

Upon neglecting the terms of higher order in t^{-1} and introducing the new time variable $T = \nu t^3[U'(y)]^{2/3}$ we may cast (34) in the standard diffusion equation form

$$\frac{\partial u}{\partial T} - \frac{\partial^2 u}{\partial \xi^2} = 0 \tag{35}$$

with the initial condition for $T = 0$

$$u = u_\infty(\xi, y, z) \tag{36}$$

which may be easily solved using standard methods. For a nonlinear source of the form (28) one obtains the simple result that the same functional behavior with ξ remains, except that l_1 is replaced by L_1, everywhere, where

$$L_1 = \sqrt{l_1^2 + 4t^3[U'(y_1)]^{2/3}} \tag{37}$$

and ϕ_o is multiplied by l_1/L_1. Thus, the long-time effect of viscosity is to make the disturbed region extend even further in the streamwise direction and to weaken the disturbance.

5. Vita-educed coherent structures

In the VITA method one averages over events for which the short-time variance

$$\mathrm{var}(u,T) = \frac{1}{T}\int_{t_e-T/2}^{t_e+T/2} u^2(t)dt - [\frac{1}{T}\int_{t_e-T/2}^{t_e+T/2} u(t)dt]^2 \tag{38}$$

exceeds a pre-selected threshold value ku_{rms}^2, where T is the integration time, k is the threshold level, selected to be typically $k \approx 1$, u_{rms}^2 is the mean-square fluctuating velocity, and where $t = t_e$ is the centered time of the event. The conditionally sampled u velocity is then usually presented as a function of the time $\tau = t - t_e$ relative to the event. The experiments show that, for a given integration time T, the normalized conditionally sampled value

$$< u >^* = < u > / \sqrt{ku_{rms}^2} \tag{39}$$

is approximately independent of the threshold parameter k and a function only of the time τ relative to the event. On the assumption that the theoretical model for the "typical" sampled event represents most of the fluctuation energy, a procedure for the model VITA event may then be outlined as follows: First, the model for the typical event is used to find the streamwise length scale, l_1, and location x behind the initial onset point which gives the maximum of the variance, var_{max}, for a given T. Then

$$< u >^* = < u > / \sqrt{var_{max} u_{rms}^2} \tag{40}$$

where $u_{rms}^2 = < u^2 >$ for the structure.

An analogous procedure can be followed for space-averaged (VISA) structures, but for the present work only VITA results were worked out.

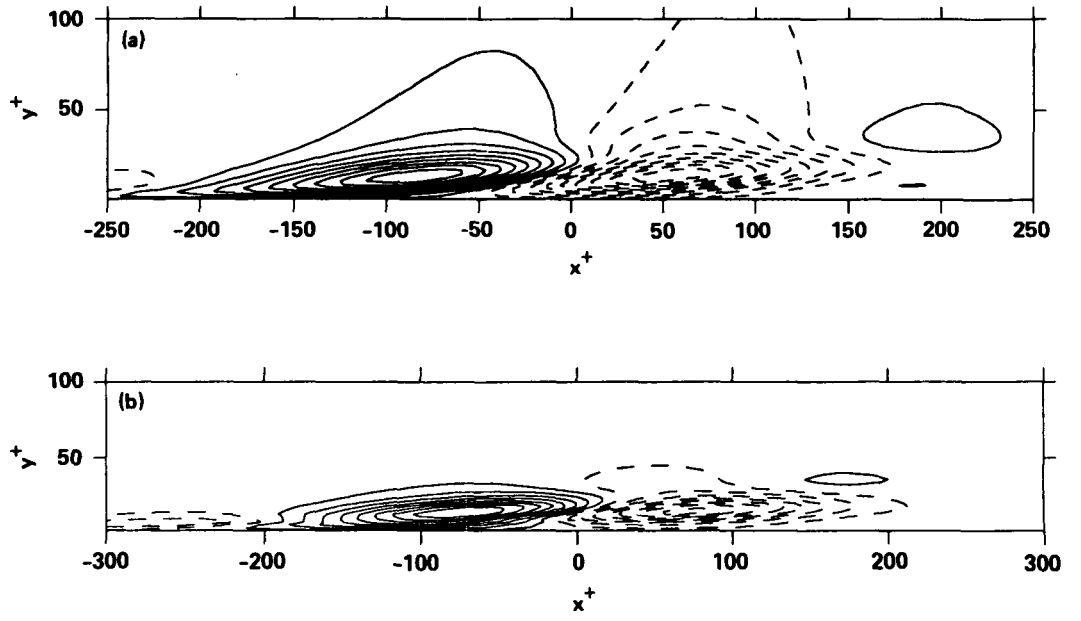

FIGURE 2. Contours of streamwise perturbation velocities in the plane $z = 0$ for model VITA-educed coherent structure at $\tau = 0$ ($t^+ = 24$) for a variance integration time of $T^+ = 20$, with $l_1 = 95$, $l_2 = 15$, $l_3 = 35$. a) Flat-eddy approximation. b)"Sausage" approximation.

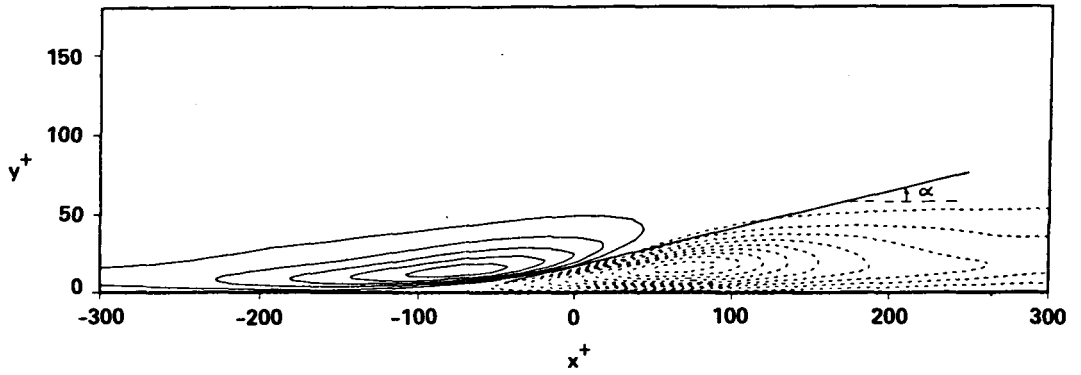

FIGURE 3. Contours of VISA-educed coherent structures with integration distance of $X^+ = 200$ obtained from numerical simulations for channel flow (from Alfredsson et al., 1988)

6. Numerical results for VITA structures

The procedure outlined above to find l_1 and x producing the highest variance for the selected integration time could be accomplished in a small numbers of trials by first selecting an initial guess of l_1 and determine for this the value of x, and the corresponding value of the integration time $T = T_m$, which yields the highest value

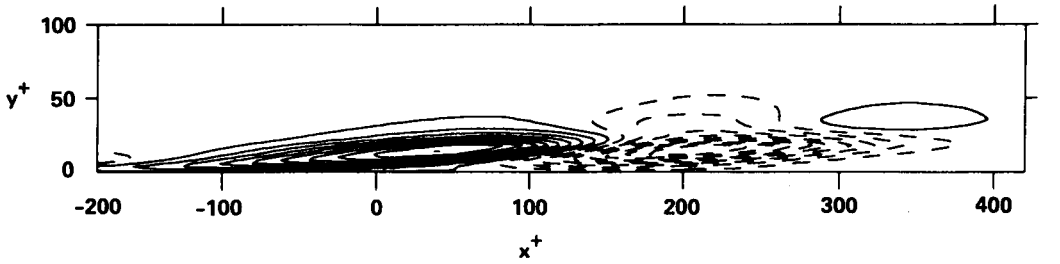

FIGURE 4. Contours of streamwise velocity perturbation at $\tau^+ = 12$ $(t^+ = 36)$ for VITA-educed eddy considered in Figure 2. "Sausage" approximation.

of the variance for the velocity scaled according to (39). A close approximation to the value of l_1 required to give the maximum for a particular desired integration time T, and the corresponding x, can then be determined simply by multiplying the original values of these quantities by T/T_m. It follows from the theory that, if viscosity is neglected, this procedure should give the correct parameter combination yielding the greatest variance for that value of the chosen averaging time. For the viscous case some small additional adjustments of the parameter values were found to be required in order to arrive at the maximum.

For the numerical evaluation of the integrals in (19) - (21), Simpson's rule was used with 20 points in the y-interval $0 - 3l_2$. The contribution from the region $y > 3l_2$ was found to be negligible. For the mean velocity distribution Reichardt's (1951) expression was employed.

Calculations were carried out for a VITA averaging time of $T^+ = 20$, applied at $y^+ = 15$, which should correspond approximately to VISA- structures obtained for an averaging streamwise distance of $X^+ = 200$, the mean velocity U at that distance from the wall being approximately 10 in viscous units. This choice was made in order to compare the results with the VISA-educed structures obtained by Alfredsson et al. (1988) from the numerical simulations for a channel flow. The procedure outlined above gave that the maximum of the normalized variance occurred at $x^+ = 225$ for $l_1^+ = 95$ at the time $t^+ = 24$ after the onset of the structure. In the calculations were used $l_2^+ = 15$ and $l_3^+ = 30$, the latter found to give a spanwise scale close to that found from the numerical simulations.

In Figure 2 the contours of constant streamwise fluctuation velocity for the coherent structure thus found in the x, y-plane are shown, both for the flat-eddy (Figure 2a) and the sausage (Figure 2b) approximations. The main qualitative difference between the two shows up for large values of y^+, which is as expected, since both approximations should hold for $y^+ \to 0$. The comparison with the VISA-structure obtained by Johansson et al (1988), see Figure 3, demonstrates that the model captures correctly the qualitative features seen in the numerical results. Thus, it shows the appearance of a high-speed upstream region separated from a low-speed downstream region by a tilted shear layer. The results for a later time, for $t^+ = 36$ (Figure 4), demonstrates that the shear layer tilts over more and more in the streamwise direction as time advances, as would indeed be the expected effect of the deformation

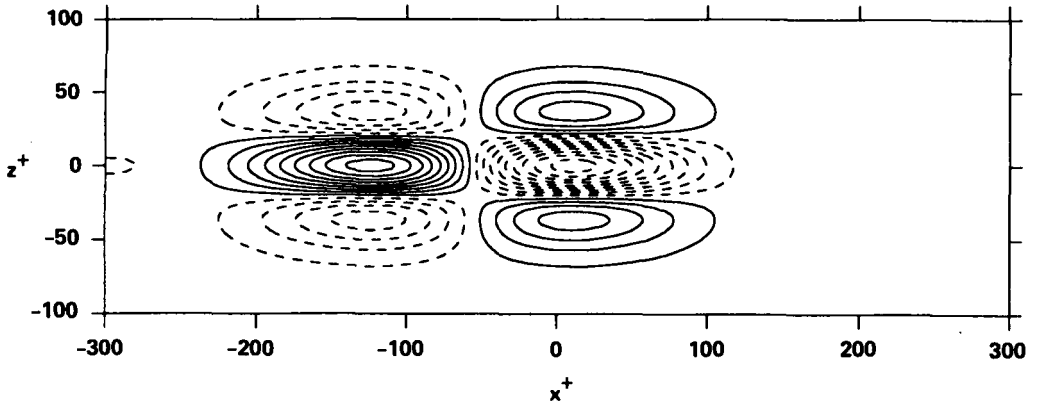

FIGURE 5. Contours at $y^+ = 15$ of streamwise velocity perturbations at $\tau^+ = 0$ according to theoretical model of Figure 2.

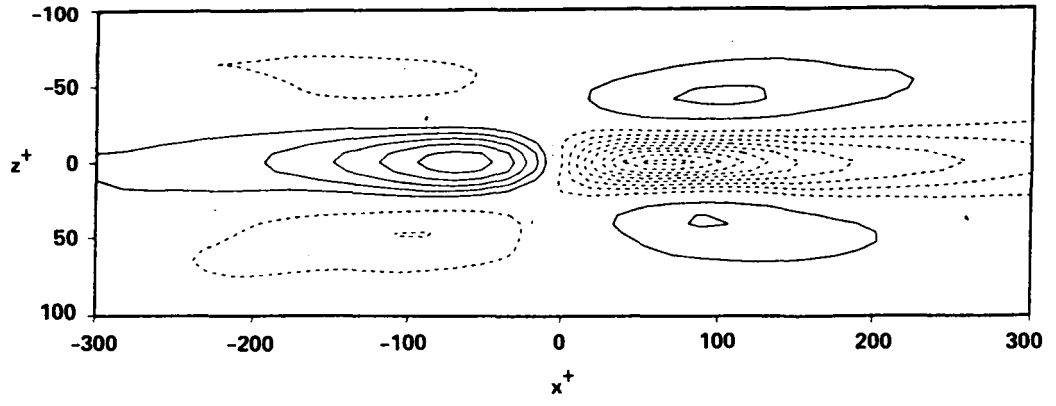

FIGURE 6. Contours at $y^+ = 15$ for VISA-educed structure from numerical simulations (from Alfredsson et al., see Figure3).

by the mean shear. The u-velocity contours in the x, z-plane for $y^+ = 15$ (Figure 5) show spanwise lobes of low velocity outside the high-velocity region and high-speed lobes outside the low-speed region, again in qualitative agreement with the results found from the numerical simulations (Figure 6). The streaky structure becomes more pronounced as time increases, as illustrated in Figure 7.

The major shortcoming of the model appears to be that it underpredicts the length of the downstream low-speed region. This could be a consequence of the assumption of an instantaneous onset of the structure. The results from the numerical simulations indicate that the onset of the bursting motion is not as abrupt as was believed earlier from the results by Kline et al. (1967), but is instead a more gradual process. Such a process, extended in time, would indeed tend to lengthen the downstream region more than the upstream one, as can be seen from (17),(18).

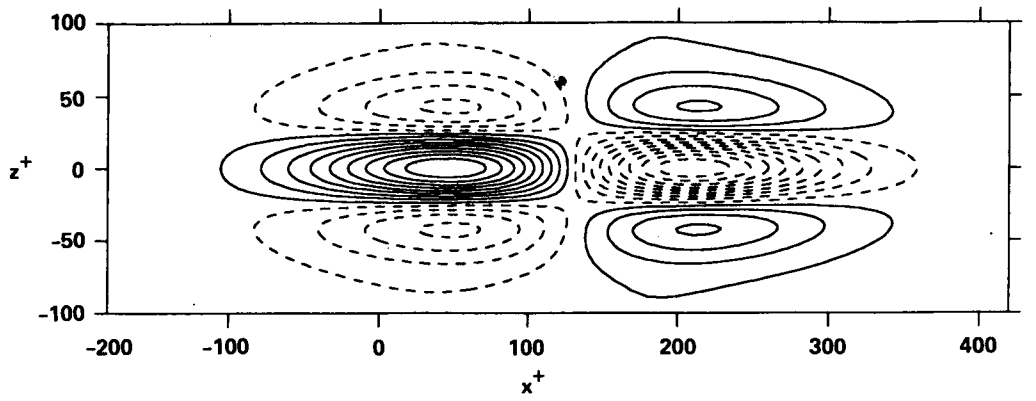

FIGURE 7. Contours of streamwise perturbation velocity for model VITA eddy (see Figure 2) at $\tau^+ = 12$.

7. Discussion and conclusions

The characteristic behavior of the VITA-educed coherent structure may be partly explained on basis of the concept of algebraic instability. From linear inviscid theory one can show (Landahl, 1980) that the kinetic energy of a localized three-dimensional initial disturbances in a parallel shear flow without any inflection point (thus being stable to wave-like disturbances according to the Rayleigh criterion) will, for a broad class of disturbances, increase linearly in time indefinitely after the onset. In the long-time behavior of the disturbance, the streamwise perturbation velocity will eventually reach a finite value, but the streamwise extent of the disturbed region will grow linearly with time, thus making the total kinetic energy, integrated over the streamwise direction, continue to grow linearly for indefinite times. Viscosity will eventually make the disturbance decay, but will take a comparatively long time to make itself felt, so that the early evolution period of the structure is likely to be dominated by inviscid mechanisms.

Further work is needed to clarify the nature of the nonlinear excitation sources. A preliminary analysis of the NASA/Ames numerical simulation data indicates (Landahl, et al. 1987) that the nonlinearity is indeed strongest in the immediate neigborhood of the wall, but the low Reynolds numbers data available to date give information only for a small range of y^+-values outside the near-wall region so that it is difficult to draw any conclusions about the behavior in the outside inviscid region.

REFERENCES

ALFREDSSON, P.H., JOHANSSON, A.V. & KIM, J. 1988 Turbulence production near walls: the role of flow structures with spanwise asymmetry. Proceedings, 2nd Summer Program of the Center for Turbulence Research. NASA Ames/Stanford University.

BLACKWELDER, R.F. & KAPLAN, R.E. 1976 On the wall structure of the turbulent boundary layer. *J. Fluid Mech.* **76**, 89.

BARK, F.H. 1975 On the wave structure of the wall region of a turbulent boundary layer. *J. Fluid Mech70.* **229.**

BREUER, K.S. 1988 The Development of a Localized Disturbance in a Boundary Layer. Mass. Inst. Tech. FDRL Report 88-1.

JOHANSSON, A.J & ALFREDSSON, P.H. 1982 On the structure of turbulent channel flow. *J. Fluid Mech.* **122**, 295.

JOHANSSON, A.V., ALFREDSSON, P.H., & ECKELMANN, H. 1987 On the evolution of shear-layer structures in near-wall turbulence. In *Advances in Turbulence* (eds. Comte-Bellot & Mathieu), Springer, 383.

KIM, H.T., KLINE, S.J. & REYNOLDS, W.C. 1972 The production of turbulence near a smooth wall in a turbulent boundary layer. *J. Fluid Mech.* **50**, 133.

KLINE, S.J, REYNOLDS, W.C., SCHRAUB, F.A. & RUNSTADLER, P.W. 1967 The structure of turbulent boundary layers. *J. Fluid Mech.* **30**, 741.

LANDAHL, M.T. 1967 A wave-guide model for turbulent shear flow. *J. Fluid Mech.* **27**, 443.

LANDAHL, M.T. 1980 A note on algebraic instability of inviscid parallel shear flows. *J. Fluid Mech98.* **243.**

LANDAHL, M.T. 1984a On the dynamics of large eddies in the wall region of a turbulent boundary layer. In *Turbulence and Chaotic Phenomena in Fluids* (ed. T. Tatsumi), Elsevier, 467.

LANDAHL, M.T. 1984b Coherent structures in turbulence and Prandtl's mixing-length theory. Z. Flugwiss. Weltraumforsch. **8**, 233.

LANDAHL, M.T., KIM, J. & SPALART, P.R. 1987 An active-layer model for wall-bounded turbulent shear flows. In *Studying Turbulence Using Numerical Simulation Databases*, NASA Report CTR-S87, 297.

LIGHTHILL, M.J. 1952 On sound generated aerodynamically. I General theory. Proc. R. Soc. London, Ser. **A211 (1107)**, 564.

PRANDTL, L. 1925 Bericht uber Untersuchungen zur ausgebildeten Turbulenz. Z. angew. Math. Mech. **5**, 136.

REICHARDT, H. 1951 Z. angew. Math. Mech. **31**, 208.

RUSSELL, J.M. & LANDAHL, M.T. 1984 The evolution of a flat eddy near a wall in an inviscid shear flow. *Phys. Fluids,27, 557.*